International Journal of
Metallurgy and Metal Physics

Preliminary Study of Carbide Dissolution during an Ultra-Fast Heat Treatment in Chromium Molybdenum Steel

M Bouzouni[1,2]* and S Papaefthymiou[1]

[1]Laboratory of Physical Metallurgy, Division of Metallurgy and Materials, School of Mining & Metallurgical Engineering, National Technical University of Athens, Greece

[2]ELKEME S.A., Viotia, Greece

Abstract

In the present work the microstructural evolution during rapid thermal cycles (< 10 sec) has been studied. For this purpose dilatometry experiments were carried out in medium carbon low alloy steel containing chromium and molybdenum (42CrMo4). Each thermal cycle of tested samples was analyzed with the use of Thermocalc® and Dictra. The microstructure was observed by means of Optical Microscopy (OM) and further characterized using Scanning Electron (SEM) and Transmission Electron Microscopy (TEM). The microstructure consists of martensite with undissolved carbides and bainitic ferrite. The results of the simulation indicate that the limited time inhibits diffusion and the alloying elements segregate at interfaces of carbides impeding their dissolution and leading to the formation of austenite with varying sizes and different carbon contents, which in some cases reach 1% wt; this means that we could get the precondition for retaining austenite at room temperature during quenching. Furthermore, we studied the effect of the chemical composition at the interfaces of austenite/carbide, ferrite/carbide, ferrite/austenite etc. and their sizes during specific temperature regions. The chemical composition for each microstructural component was selected with the use of Thermo calc.

Introduction

Steel development in the last two decades was driven by the need of the automotive industry to face the challenge of complying with the passenger's safety standards while maintaining fuel efficiency and minimizing emissions. The most promising route to achieve these objectives is to minimize the overall car weight. For this purpose as far as steel concerned, the family of Advanced High Strength Steels has been developed with increased mechanical properties than conventional steels [1,2]. The need for weight reduction is nowadays even more significant as we move along an emission free transportation with the replacement of combustion engines from electric ones. Batteries add significantly to the overall car weight. This is why OEMs introduce into their Body-In-White (BIW) light alloys (e.g. Aluminium and Magnesium) and Carbon Reinforced Plastics (CRP). Steel remains significantly cost effective in comparison to such solutions. But in order to be competitive, even higher strength is needed. A good combination of strength and ductility can be achieved via ultra-fine grained nano-precipitated hardened phases, mainly ferritic and bainitic mixtures of retained austenite with martensite, and strengthening mechanisms such as solid solution, carbide precipitation causing dislocation generation and slip and transformation or twinning during deformation [3-10].

***Corresponding author:** *M Bouzouni, Laboratory of Physical Metallurgy, Division of Metallurgy and Materials, School of Mining & Metallurgical Engineering, National Technical University of Athens, 9, Her. Polytechniou str., Zografos, Athens, 15780, Greece; ELKEME S.A., 56th km Athens-Lamia Nat. Road, 32011 Oinofyta, Viotia, Greece, E-mail: mbouzouni@elkeme.vionet.gr*

Received: March 25, 2017: **Accepted:** July 13, 2017: **Published:** July 15, 2017

Citation: Bouzouni M, Papaefthymiou S (2017) Preliminary Study of Carbide Dissolution during an Ultra-Fast Heat Treatment in Chromium Molybdenum Steel. Int J Metall Met Phys 2:005

Another promising approach to achieve high strength with increased ductility has led to the development of flash processing i.e. rapid heating, short holding time at the austenization temperature and quenching which results in mixed microstructures of martensite-bainitic ferrite and carbides exhibiting superior mechanical properties than advanced high strength steels (e.g. 1,4-1,5 GPa for Yield Strength (YS), 1,8-2,0 GPa for Tensile Strength (TS) and 5-8% for total elongation) [11-13]. The increase of heating rate and the initial microstructure affect significantly recrystallization and austenite decomposition [14-16]. Nevertheless, the understanding of the mechanisms that exist at ultra-fast thermal cycle will lead in the development of a new alloy free from expensive additions with mechanical properties adequate of AHSS produced in one step.

The purpose of the present work is to study the carbide dissolution and phase transformations during an Ultra-Fast Heat Treatment (UFHT). The lack of time for diffusion contributes to a heterogeneous element distribution along interfaces and leads to a refined and complex final microstructure. In order to understand and control these microstructures we use dilatometry to apply rapid thermal cycles, STEM to characterize the ultra-fine microstructures (phases, type and morphology of carbides) and EDS to define the composition of precipitates and the chemical heterogeneity within the microstructure. Thermocalc® and DICTRA [17] serve our efforts to study in depth the migration of alloying elements and the carbide dissolution during ultra-fast heating and isothermal holding at peak temperature when this time is not available and to explain the microstructural evolution under rapid thermal treatment.

Materials and Methods

Material and ultra-fast heat treatment

In order to examine the evolution of microstructure under rapid thermal cycles, typical soft annealed medium carbon chromium molybdenum steel was used with spheroidized carbides (Table 1). Ultrafast heat treatment was applied using dilatometry. Dilatometric plate and round samples (plate sizes length 10 mm with width 2 mm; round sizes: length 10 mm with diameter of 3 mm) derived from cross sections cut out of hot rolled bars with dimensions 95 × 49 × 5500 mm^3 (width × thickness × length). Chemical composition analysis was performed in 30 × 30 mm^2 cross sections of the bars, transverse to rolling direction by means of Optical Emission Spectroscopy (OES). Cylindrical as well as non-Standard dilatometric plate specimens were machined using Wire Electro-Discharge Machining (EDM) with dimensions 2 × 4 × 10 mm^3. The nonstandard specimens allow higher heating and cooling rates to be achieved, critical for the present heat treatment cycle. EDM was used to assure that the dimensions have low tolerance and at the same time the microstructure remains intact. The dilatometry tests were performed in a Bähr 805A Quench dilatometer. The apparatus uses an induction coil to heat the sample and detects the length change of the sample with a Linear Variable Displacement Transducer (LVDT). The specimens were placed in the dilatometer with a thermocouple spot welded at the middle in order to control the temperature. Experiments with two thermocouples were also performed, one at the edge and the second at the middle in order to check the temperature gradient and, thus, to make sure that the transformations occur in the whole sample and not just in the middle. It was found, that for the nonstandard specimens, even though the sample cross section was not cylindrical, the temperature variation margin was within 10 °C. All samples were heated at 200 °C/sec to peak temperature (950 °C) under vacuum and then quenched with helium at the same rate to room temperature. The treatment included no isotheral holding time at the austenitization temperature.

Table 1: Chemical analysis of CrMo-steel (in wt. - %).

C	Mn	Si	P	S	Cr	Mo
0.407	0.79	0.21	0.009	0.010	0.97	0.187

Microstructural characterization

The microstructure was studied with Optical Microscopy (OM) and subsequently with Transmission Electron Microscopy (TEM) were conducted with a high resolution JEOL JEM-2100, operating at 200 kV, equipped with an Oxford Energy-Dispersive X-ray Spectroscopy (EDS) microanalysis system. Samples were prepared according to the standard procedure, i.e., by grinding and polishing to 1 μm diamond paste. Chemical etching for revealing in a first step the microstructure was performed with Nital 2%. Afterwards, the same sample preparation was repeated and the etching was performed this time with 10% aqueous sodium metabisulphite tint etching solution. The aim was to reveal the multiphase microstructure and to distinguish the areas of interest (e.g. carbides, retained austenite, bainitic ferrite) for the higher magnification techniques. Disk specimens for TEM were cut from the dilatometry samples, manually ground to a thickness of 80 μm and then the final thinning was carried out with Precision Ion Polishing System (PIPS).

Modeling

Thermodynamic and kinetic calculations were performed with Thermocalc (TCFE8) and DICTRA (TCFE8, MOBFE3) software respectively. The simulation was based on the phase diagram (Figure 1) of the material and dilatometry results such as heating rate and dwelling time. In the simulation, the diffusion of alloying elements was studied at the interfaces of carbides (e.g. cementite, M_7C_3) with ferrite and austenite from 513 °C up to 950 °C (Table 2). For this purpose the ini-

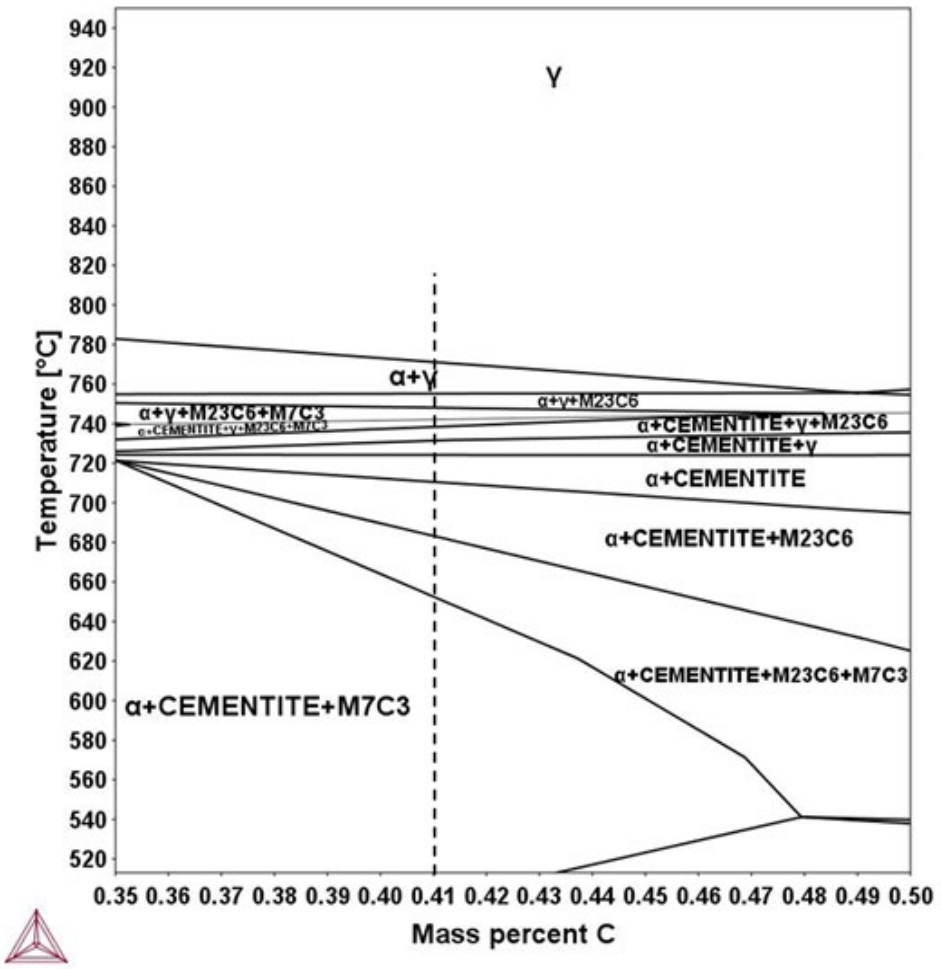

Figure 1: Phase diagram of CrMo steel calculated using Thermocalc® software. The dashed line indicates the carbon concentration of 42CrMo4.

Table 2: Table of the temperature ranges and systems studied in conjunction with the dilatometry results.

	513-633 °C	633-728 °C	728-810 °C	810-900 °C	900-950 °C	950 °C Isothermal
Studied systems	Cementite/ Ferrite M_7C_3/Ferrite	Cementite/ Ferrite M_7C_3/Ferrite $M_{23}C_6$/Ferrite	Cementite/ Ferrite M_7C_3/Ferrite $M_{23}C_6$/Ferrite	Cementite/Austenite/ Ferrite M_7C_3/Austenite/Ferrite	Cementite/ Austenite M_7C_3/Austenite	Cementite/Austenite M_7C_3/Austenite
Heating rate (°C/sec)	274.1	727.04	191.3	238.94	187.6	0
Dwelling time (sec)	0.44	0.131	0.43	0.376	0.266	1.8

tial size of carbides was set at 5 nm with spherical geometry and we assume that local equilibrium holds at the interfaces of carbides with ferrite and austenite.

Results

Microscopy (OM and TEM) results

The results from OM show the microstructure is extremely refined. Using the tinting etching technique we expect to view martensite in brown and bainitic ferrite in blue, while carbides will appear white [18,19] (Figure 2).

The TEM analysis revealed that the microstructure after the UFHT consists of martensite laths (20-50 nm width and 500-1000 nm length) and bainitic ferrite as well as spherical carbides ranging from 5 nm to 500 nm (Figure 3, Figure 4 and Figure 5). In Figure 4 the elongation of the carbide is due to the limited diffusion at increased temperatures. In addition, shaded rings are observed inside the carbide. These rings are produced by mass contrast effect possibly consequence of the diffusion of substitutional alloying elements during carbide dissolution. These carbides are either chromium carbides or cementite enriched in chromium. Finally, in the microstructure after the UFHT the TEM-EDS analysis

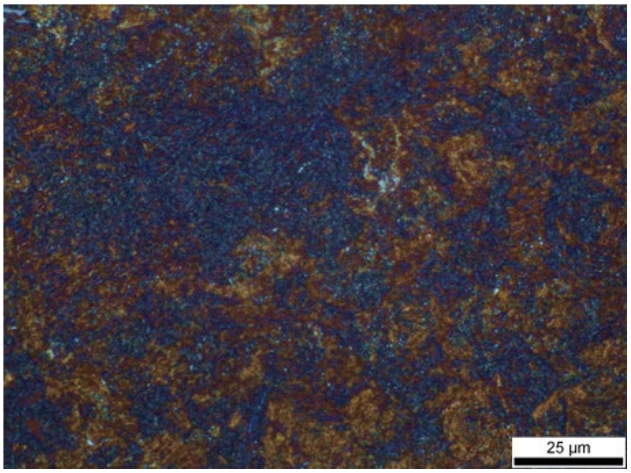

Figure 2: Microstructure consisting of bainitic ferrite (blue area) and martensite (brown area) and carbides (white areas).

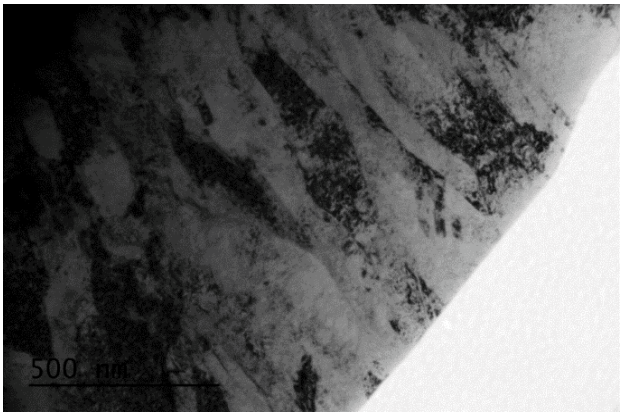

Figure 3: TEM micrograph (bright field) of a microstructure gained after UFHT (with heating rate 200 °C/s, peak austenitization for less than 3 s and helium quenching with cooling rate similar to water quenching). In the microstructure, martensite coexists with bainitic ferrite and carbides.

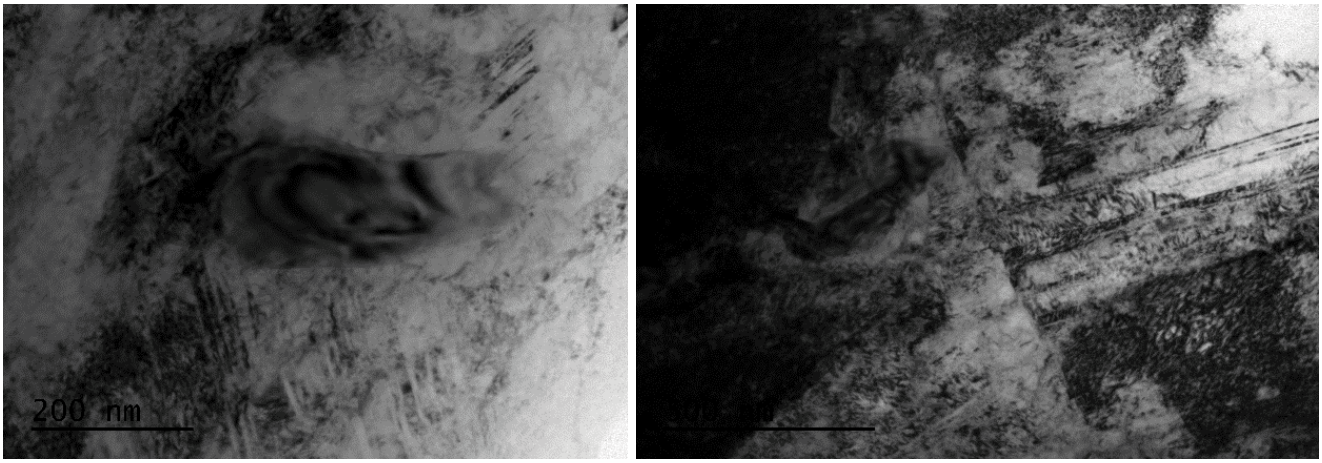

Figure 4: TEM micrograph of microstructure after UFHT a) Chromium carbide in the microstructure after UFHT; b) Chromium enriched cementite at interfaces.

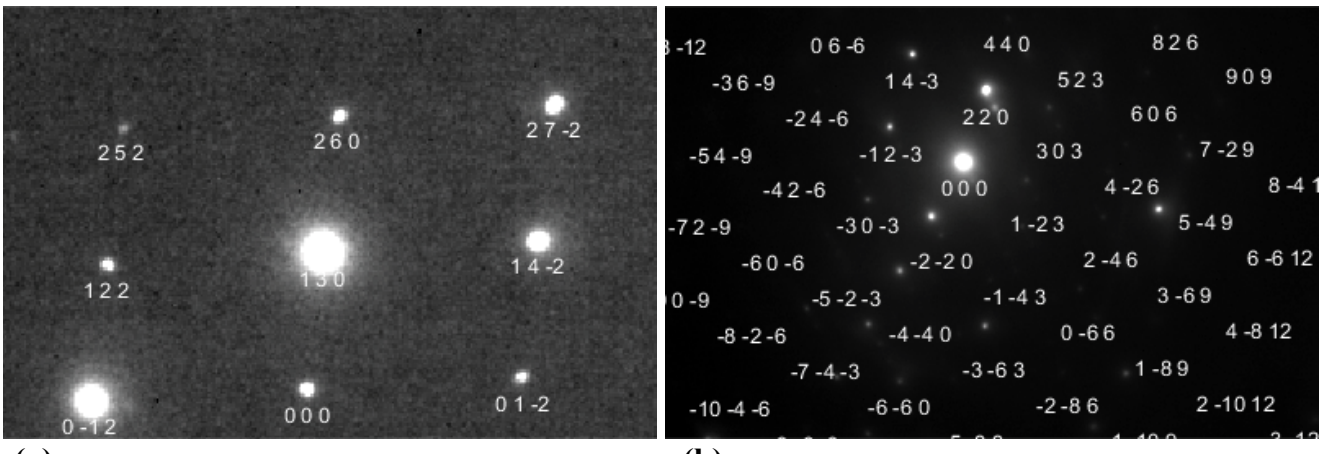

Figure 5: Indexed pattern of Figure 4, a) Chromium carbide of the type Cr7C3; b) Chromium cementite [20].

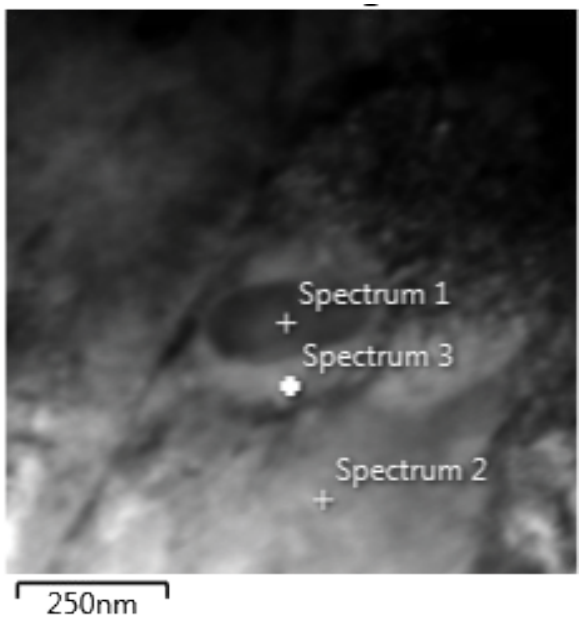

Figure 6: Scanning TEM micrograph of carbides in the microstructure after UFHT showing the spots of the EDS analysis.

shows that there is chemical heterogeneity in the microstructure (Figure 6 and Table 3).

Modeling results

The results of the simulation (Figure 7, Figure 8 and Figure 9) indicate that due to the limited time the diffusion is inhibited and alloying elements such as chromium segregate at the interfaces of carbides within the matrix. This increase impedes the dissolution of carbides and leads to formation of regions poor (0.4% wt C) and rich in carbon (~1% wt C) in austenite at peak temperature.

Discussion

The initial microstructure of the sample is soft annealed with spheroidized carbides. Slow heating can

Table 3: TEM - EDS spot chemical analysis in the microstructure after UFHT of Figure 6.

STEM - EDS spot analysis	Cr	Mn	Fe
Spectrum 1	23.24	8.32	rest
Spectrum 2	0.95	1.02	rest
Spectrum 3	5.12	5.22	rest

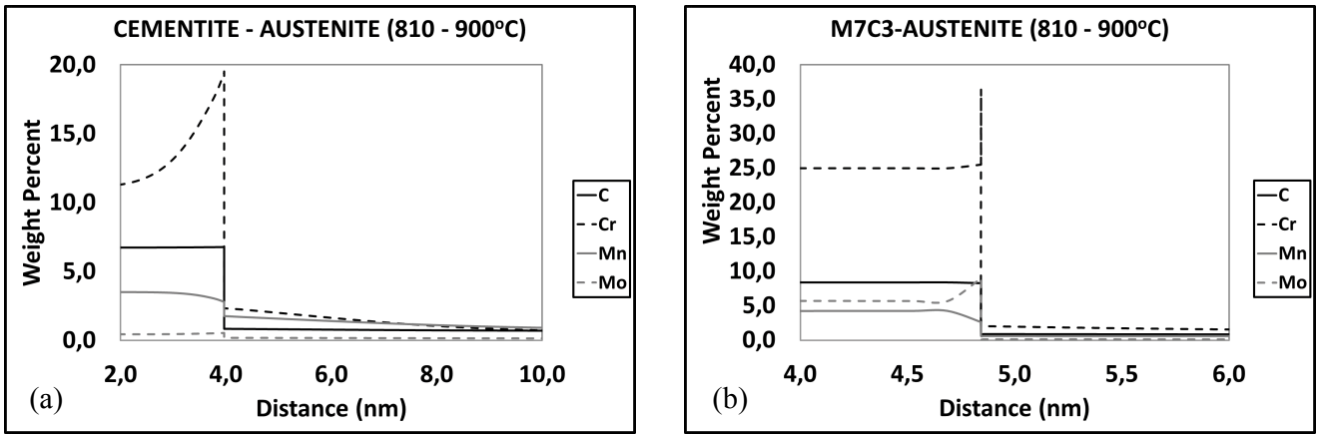

Figure 7: a) Chemical composition at the interface of cementite with austenite; b) Chemical composition of M_7C_3 carbide with austenite at the inter-critical region of 810 °C and 900 °C.

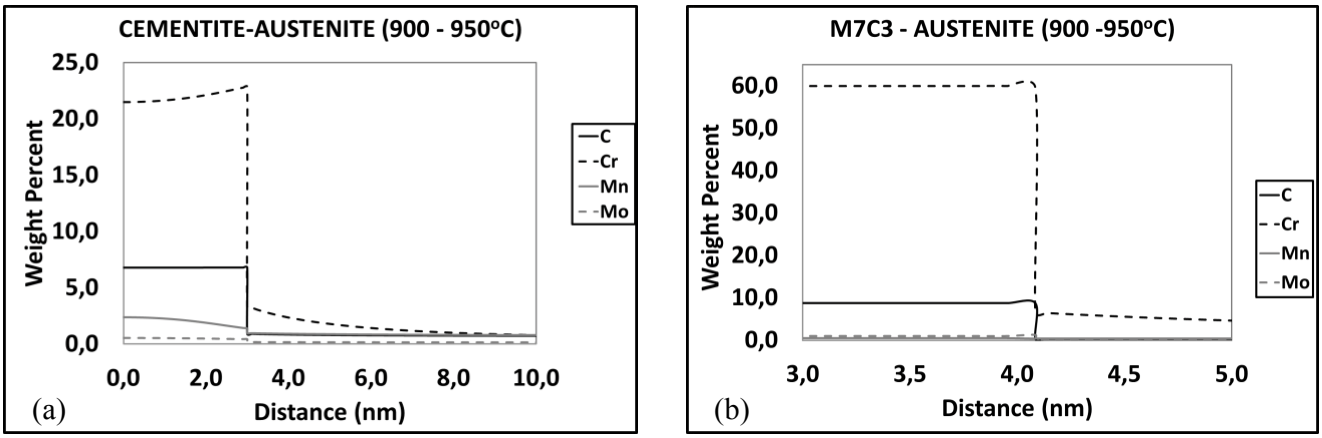

Figure 8: a) Chemical composition at the interface of cementite with austenite; b) Chemical composition of M_7C_3 carbide with austenite at the region of 900 °C and 950 °C.

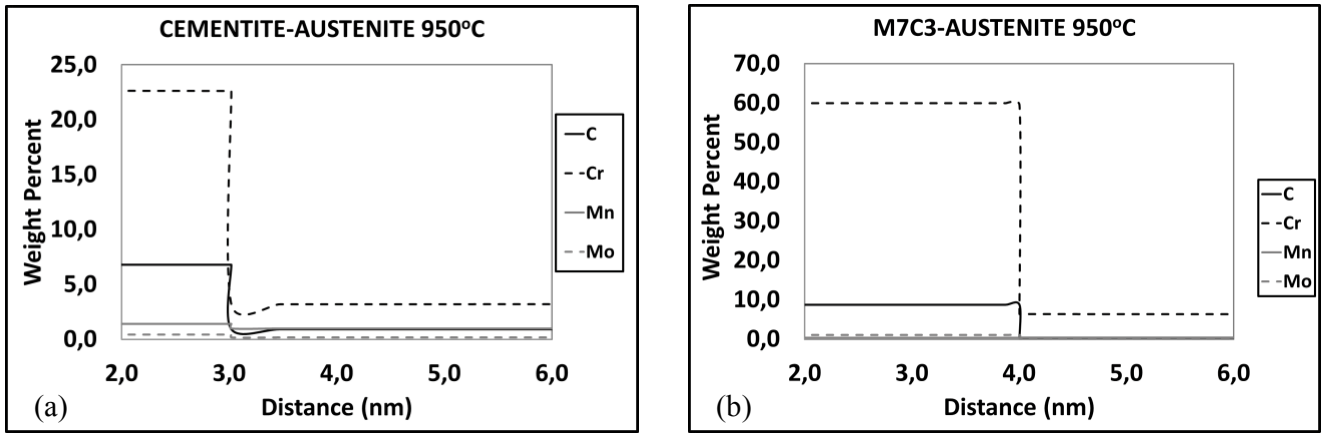

Figure 9: a) Chemical composition at the interface of cementite with austenite; b) Chemical composition of M_7C_3 carbide with austenite at the region of 950 °C.

support the diffusional progress of manganese and chromium positioning at favorable locations within the microstructure. In case of rapid heating rate (> 200 °C/s) the diffusion of alloying elements is restricted especially those with larger atomic radius such as Chromium (Cr) and Manganese (Mn). However, a partitioning of alloying elements is observed at 2-D defects such as interfaces between carbides and austenite [20,21]. The segregation of alloying elements at interfaces locally alters the chemical composition contributing to chemical heterogeneity. The gradient of alloying elements such as Chromium (Cr) and Manganese (Mn) limits the dissolution of carbides. The undissolved carbides act as nucleation sites, thus, leading to an exceptionally refined microstructure. Moreover, the undissolved carbides as well as the segregation of alloying elements at grain boundaries affects phase transformations such as bainitic ferrite and martensite. Segregation depends on misorientation between grains and dislocations in the microstructure [22]. The higher the misorientations angle at grain boundaries, the more intense the segregation. Dislocations at the triple points of grain boundaries or in the proximity of undissolved carbides act as additional sites for segregation, thus, enhancing micro-diffusion in these regions. Finally, the limited time at the austenization temperature not only restricts the austenite growth, but also ensures the chemical heterogeneity due to limited time for diffusion.

Conclusions

As a conclusion to this work, it has been observed that rapid thermal cycle restricts diffusion of alloying elements, thus, leading to segregation of alloying elements in 2-D defects such as grain boundaries-interfaces and defects in the microstructure. The local increase of alloying elements in the interface of carbides controls the dissolution of carbides and the chemical heterogeneity in the microstructure. The undissolved carbides and the limited time at peak temperature prevent grain growth of austenite, thus, leading to refined microstructure. The chemical heterogeneity in austenite, in terms of carbon, strongly influences phase transformations in quenching thus leading in mixture of phases with bainite and martensite. However the simulation results show strong evidence for retained austenite in the final microstructure, which was not found in TEM. Therefore, further investigation in the effect of chemical composition and size of austenite during and after the bainitic and martensitic transformation is necessary, as well as a thorough study on the effect of the alloying elements on the transformations mentioned.

References

1. W Bleck (2002) TRIP-Aided High Strength Ferrous Alloys. Ghent, Belgium.
2. W Bleck, A Frehn, S Papaefthymiou (2004) Microstructure and tensile properties in DP and TRIP steels. Materials Technology - TRIP Steels 75: 704-710.
3. G Frommeyer, O Grässel (2002) High Strength and Ultra - Ductile FeMn(Al,Si)TRIP/TWIP light-weight steels for structural components in automotive engineering. Stahl Und Eisen 122: 65-69.
4. VF Zackay, ER Parker, D Fahr, R Bush (1967) The enhancement of ductility in high-strength steels. Transactions of the ASM 60: 252-257.
5. FG Caballero, HW Yen, MK Miller, JR Yang, J Cornide, et al. (2011) Complementary use of transmission electron microscopy and atom probe tomography for the examination of plastic accommodation in nanocrystalline bainitic steels. Acta Materialia 59: 6117-6123.
6. M Calcagnotto, Y Adachi, D Ponge, D Raabe (2011) Deformation and fracture mechanisms in fine-and ultrafine-grained ferrite/martensite dual-phase steels and the effect of aging. Acta Materialia 59: 658-670.
7. Carlos Garcia Mateo, H Bhadeshia (2004) Nucleation theory for high-carbon bainite. Materials Science and Engineering: A 378: 289-292.
8. C Garcian Mateo, F Caballero, H Bhadeshia (2003) Development of hard bainite. ISIJ International 43: 1238-1243.

Citation: Bouzouni M, Papaefthymiou S (2017) Preliminary Study of Carbide Dissolution during an Ultra-Fast Heat Treatment in Chromium Molybdenum Steel. Int J Metall Met Phys 2:005

9. C Garcia-Mateo, F Caballero, T Sourmail, M Kuntz, J Cornide, et al. (2012) Tensile behaviour of a nanocrystalline bainitic steel containing 3wt% silicon. Materials Science and Engineering: A 549: 185-192.

10. B Hutchinsona, J Hagström, O Karlsson, D Lindell, M Tornberg, et al. (2011) Microstructures and hardness of as-quenched martensites (0.1-0.5%C). Acta Materialia 59: 5845-5858.

11. G Cola (2007) Properties of bainite nucleated by water quenching in 80 ms. Tokyo.

12. T Lolla, G Cola, B Narayanan, B Alexandrov, S Babu (2011) Development of rapid heating and cooling (flash processing) process to produce advanced high strength steel microstructures. Material Science and Technology 27: 863-875.

13. T Lolla, B Alexandrov, S Babu, G Cola (2009) Towards understanding the microstructure development during flash heating and cooling of steels. Berlin, Germany.

14. FC Castro, C Goulas, I Sabirov, S Papaefthymiou, A Monsalve, et al. (2016) Microstructure, texture and mechanical properties in a low carbon steel after ultra fast heating. Materials Science & Engineering A 672: 108-120.

15. FC Castro, B Schulz, S Papaefthymiou, A Artigas, A Monsalve, et al. (2016) The Effect of Ultrafast Heating on Cold-Rolled Low Carbon Steel: Formation and Decomposition of Austenite. Metals 6: 1-14.

16. FC Castro, I Sabirov, C Goulas, J Sietsma, A Monsalve, et al. (2017) Austenite formation in 0.2% C and 0.45% C steels under conventional and ultrafast heating. Materials and Design 116: 448-460.

17. J Andersson, T Helander, L Höglund, P Shi, B Sundman (2002) Thermo-Calc and DICTRA, Computational tools for materials science. Calphad 26: 273-312.

18. H Zakerinia, A Kermanpur, A Najafizadeh (2009) Color metallography; A suitable method for characterization of martensite and bainite in multiphase steels. International Journal of Iron and Steel Society of Iran 6: 14-18.

19. CK Shui, WT Reynolds, GJ Shiflet, HI Aaronson (1988) A Comparison of Etchants for Quantitative Metallography of Bainite and Martensite Microstructures in Fe - C - Mo alloys. Metallography 21: 91-102.

20. Miloslav Klinger, Aleš Jäger (2015) Crystallographic Tool Box (CrysTBox): automated tools for transmission electron microscopists and crystallographers. J Appl Crystallogr 48: 2012-2018.

21. C Philippot, K Hoummada, M Dumont, J Drillet, V Hebert, et al. (2015) Influence of a 2-D defect on the partitioning during the formation of a cementite particle in steels. Computational Materials Science 106: 64-68.

22. D Raabe, M Herbig, S Sandlöbes, Y Li, D Tytko, et al. (2014) Grain boundary segregation engineering in metallic alloys: A pathway to the design of interfaces. Current Opinion in Solid State and Materials Science 18: 253-261.

Citation: Bouzouni M, Papaefthymiou S (2017) Preliminary Study of Carbide Dissolution during an Ultra-Fast Heat Treatment in Chromium Molybdenum Steel. Int J Metall Met Phys 2:005